INSTITUTE OF PLASMA PHYSICS

NAGOYA UNIVERSITY

Wave Trajectory and Electron Cyclotron Heating
in Toroidal Plasmas

T. Maekawa, S. Tanaka, Y. Terumichi and Y. Hamada

IPPJ-313 December 1977

RESEARCH REPORT

NAGOYA, JAPAN

Wave Trajectory and Electron Cyclotron Heating in Toroidal Plasmas

T. Maekawa, S. Tanaka, Y. Terumichi and Y. Hamada

IPPJ-313 December 1977

Further communication about this report is to be sent to the Research Information Center, Institute of Plasma Physics, Nagoya University, Nagoya 464, Japan

---

Permanent address : Department of Physics, Kyoto University, Kyoto 606, Japan

Abstract

Wave trajectories propagating obliquely to magnetic field in toroidal plasmas are studied theoretically. Results show that the ordinary wave at appropriate incident angle is mode-converted to the extraordinary wave at first turning point and is further converted to the electron Bernstein wave during passing a loop or a hooked nail curve near second turning point and is cyclotron-damped away, resulting in local electron heating, before arriving at cyclotron resonance layer.

Recently the experiments on the electron cyclotron heating (ECH) in tokamaks,[1,2] Octupole[3] and the Elmo bumpy torus[4] have recieved considerable attentions in connection with possibility of further heating and modification of current profile,[5] which may be possible by development of the gyrotron.[6] In toroidal devices, plasma parameters such as electron density and magnetic field are strongly nonuniform, so that such studies as wave propagation, mode conversion and absorption are very important in order to succeed in these ECH experiments. It is suggested theoretically that by injecting microwave in the direction of decreasing major radius in the toroidal plasma the extraordinary (X) mode is excited, then, after penetrating the evanescent region due to the cyclotron cutoff, the X-mode reaches the upper hybrid resonance (UHR) layer ($\omega = \omega_{UH} = \sqrt{\omega_{pe}^2 + \Omega_e^2}$), where the X-mode is converted into the electron Bernstein wave.[7,8,9] Further, the wave propagates to the electron cyclotron resonance (ECR) layer ($\omega = \Omega_e$), where the wave is cyclotron-damped. In order to avoid the wave reflection ascribed to the cyclotron cutoff, it is planned to inject the microwave in the direction of increasing major radius.[2,5] On the contrary, it was suggested by Preinhaelter et al.[10] that in a plasma with varying density in an uniform magnetic field, the ordinaly (O) mode propagating at an appropriate angle to the field is transformed into the X-mode near the plasma cutoff ($\omega = \omega_{pe}$).

In this report, we first present the wave trajectries (group velocity trajectories) of the wave propagating in toroidal plasmas, where the obliquely propagating O-mode is converted into the

X-mode and then into the electron Bernstein mode, and finally is cyclotron-damped in front of ECR layer. The studies of these trajectories are essentially important not only for the ECH experiments, but also for measurements on the electron cyclotron emission from tokamak plasmas[11] and the cyclotron emission loss in a reacter.

At first, we shall study the dispersion of electromagnetic waves in a plasma slab model with a density gradient along the x-direction in a magnetic field $\vec{B}$ along z-direction. Assuming that non-uniformities of plasma parameters are weak and the geometrical optics is valid, the dispersion equation of wave with a constant refractive index $N_z=ck_z/\omega$ along z-direction at a local position (x,z) is given by[12]

$$\varepsilon(\omega, \vec{k}) = aN_\perp^4 - bN_\perp^2 + c = 0 \qquad (1)$$

in the cold plasma approximation, where $a=S$, $b=RL+PS-(P+S)N_z^2$ and $c=P(RL-2SN_z^2+N_z^4)$ (R, L, P and S are the Stix's notations[12] and only electron terms should be retained).

In Fig. 1 are plotted the refractive index $N_\perp$ perpendicular to $\vec{B}$ as functions of ω_{pe}^2/ω^2 for the various values of N_z at a fixed value of Ω_e/ω. While, O- and X-modes do not intersect in the case of $N_z=0$, their dispersion curves are connected in the imaginary region for a small value of N_z (excluding the point at $\omega_{pe}^2/\omega^2=0$). As N_z increases, this evanescent region decreases and at last disappears at $N_z=N_{z,opt}=[\Omega_e/(\omega+\Omega_e)]^{1/2}$, or at the incident angle $\theta_{opt}=\arccos N_{z,opt}$.[10] For $N_z > N_{z,opt}$, there appears the evanescent region in a low

density side ($\omega_{pe}/\omega<1$). In a rather wide range of N_z around $N_z=N_{z,opt}$, the transmission coefficient of O-mode through this evanescent layer is shown to be nearly unity, since the layer is narrow and shallow ($|N_z|\ll 1$). It is also shown that the transmitted O-mode are fully transformed into the X-mode at the first turning point,[10] $(\omega_{pe}/\omega)^2=1+[(\Omega_e/\omega)(1-N_z^2)/2N_z]^2$. The converted X-mode propagates back in the low density side and reaches UHR layer, where the cold plasma approximation is invalid and the thermal effects of electrons must be taken into account.

Assuming the maxwellian velocity distribution, we can write the exact dispersion equation for the hot plasma wave as follows:[13]

$$\varepsilon(\omega, \vec{k}) = \det\left|\overleftrightarrow{K} - N^2(\overleftrightarrow{I} - \vec{N}\vec{N}/N^2)\right| = 0, \qquad (2)$$

where $\overleftrightarrow{K}$ is the dielectric tensor at the local position and it is written as follows,

$$K_{ij}(\omega, \vec{k}) = \delta_{ij} - \frac{\omega_{pe}^2}{\omega^2}\left\{\sum_{n=-\infty}^{+\infty}\frac{\zeta_0}{\zeta_n}\Gamma_{ij}[1+Z'(\zeta_n)/2]-2\zeta_0^2\hat{z}\hat{z}\right\},$$

where

$$\Gamma_{ij} = \begin{Bmatrix} \frac{n^2}{\lambda}\Lambda_n(\lambda) & in\Lambda_n'(\lambda) & \sqrt{2\lambda}\,n\zeta_n\Lambda_n(\lambda) \\ -in\Lambda_n'(\lambda) & \frac{n^2}{\lambda}\Lambda_n(\lambda)-2\lambda\Lambda_n'(\lambda) & -i\sqrt{2\lambda}\,\zeta_n\Lambda_n'(\lambda) \\ \sqrt{2\lambda}\,n\zeta_n\Lambda_n(\lambda) & i\sqrt{2\lambda}\,\zeta_n\Lambda_n'(\lambda) & 2\zeta_n^2\Lambda_n(\lambda) \end{Bmatrix},$$

$\Lambda_n(\lambda)=e^{-\lambda}I_n(\lambda)$, $\Lambda_n'(\lambda)=d\Lambda_n/d\lambda$, $\lambda=k_\perp^2T_e/m_e\Omega_e^2=k_\perp^2\rho_e^2/2$, $sgn\sqrt{\lambda}=k_\perp/|k_\perp|$, $\zeta_n=(\omega-n\Omega_e)/k_z v_{Te}$ and $Z'(\zeta_n)$ is

the first derivative of the plasma dispersion function.

If $N^2=N_\perp^2+N_z^2$ is large considerably, the electrostatic approximation is valid and the following electron Bernstein wave is obtained by the equation, $\mathcal{E}=\vec{k}\cdot\overleftrightarrow{K}\cdot\vec{k}/\,k^2$:[12]

$$\mathcal{E}(\omega,\vec{k}) = 1-\frac{2\omega_{pe}^2}{k^2v_{Te}^2}\sum_{n=-\infty}^{+\infty}\left\{\frac{n\Omega_e}{\omega-n\Omega_e}+\frac{\omega}{\omega-n\Omega_e}\frac{Z'(\zeta_n)}{2}\right\}\Lambda_n(\lambda)=0. \quad (3)$$

In Fig. 2 are plotted the three kinds of $N_\perp$ as functions of ω_{pe}^2/ω^2 calculated from eqs.(1), (2) and (3), respectively, with the various values of T_e for $N_z=N_{z,opt}$. It is reasonable that the exact dispersion curve (ABCDJK for T_e=1.6 keV) is well approximated that of the cold X-mode if $N_\perp \lesssim 1$, while it is by that of Bernstein mode if $N_\perp \gtrsim 5$. In the intermediate range of $N_\perp$, the exact dispersion curve should be calculated, since the discrepancy between both solutions becomes large with the increasing T_e

In accordance with the variation of $N_\perp$ in Fig. 2, we calculate the wave trajectory, $\vec{r}(t)$, determined from the following set of differential equations,[12,14]

$$\frac{d\vec{r}}{dt} = -\frac{\partial\mathcal{E}/\partial\vec{k}}{\partial\mathcal{E}/\partial\omega} = \vec{v}_g, \quad \frac{d\vec{k}}{dt} = \frac{\partial\mathcal{E}/\partial\vec{r}}{\partial\mathcal{E}/\partial\omega}, \quad (4)$$

where $\mathcal{E}(\omega,\vec{k})=0$ is the local dispersion equation given by eqs.(1), (2) or (3), assuming that ω is constant along the trajectory. When the plasma is homogeneous along the z-direction, it is shown from eq.(4) that k_z is a constant along the trajectory, which is the reason why we take N_z= const. in the calculation of dispersion curves.

For the computer calculations of the wave trajectories in the equatorial plane of torus, the plasma is simulated by the plasma slab model, where the electron density and the magnetic field are varied as follows:

$$\frac{\omega_{pe}^2(x)}{\omega^2} = \frac{\omega_{pe}^2(0)}{\omega^2}\left(1-\frac{x^2}{a^2}\right), \qquad \frac{\Omega_e(x)}{\omega} = \frac{\Omega_e(0)}{\omega}\,\frac{R}{R-x}, \quad (5)$$

where, R (a) is the major (minor) radius of the torus, and $\omega_{pe}(0)$ and $\Omega_e(0)$ are the respective values at the magnetic axis (x=0) [Fig. 3(a)]. Though the magnetic field as well as the density are varied, the variation of $N_\perp(x)$ is rather similar to that in an uniform B (Fig. 2), except in the vicinity of ECR layer.

In Figs. 3(b) and (c) are plotted the wave trajectories calculated from eqs.(2) and (4) in the case of $N_z=N_{z,opt}$ at the plasma cutoff. Being injected at the plasma boundary (point A) at the incident angle θ_{opt}, the O-mode propagates to the plasma cutoff point (B), where $N_\perp=0$ and $\vec{k}//\vec{B}$, then the O-mode propagates in a backward wave for the X-directior to the first turning point (C), where the group velocity perpendicular to $\vec{B}$, $v_{g\perp}=0$, and the O-mode is converted to the X-mode. At the point D, the group velocity parallel to $\vec{B}$, v_{gz} is inverted, and the X-mode propagates in a backward wave for the z-direction toward the second turning points (E,M,J), where the wave trajectories show the interesting, but complicated behaviours, that is, the trajectory passes the loop, DEI, in

a low T_e plasma, while it does the hooked nail curve, DJK, in a high T_e plasma. As $\omega_{pe}(0)/\omega$ increases, the transmitted distances AC and AE become short. On the other hand, if the density is low (for example, $\omega_{pe}^2(0)/\omega^2 = 1.1223$), there is no mode-conversion point after penetrating the plasma cutoff and the O-mode is reflected back toward the boundary.

In a cold plasma approximation, the X-mode propagates to the UHR layer, F, where $N_\perp \to \infty$ and $\vec{v}_{g\perp} \vec{v}_{ph} = (\omega/|k|^2)\vec{k}$ and the trajectory is parallel to $\vec{B}$, while in an electrostatic approximation the Bernstein wave propagates along the trajectory GHI, and the exact trajectory is given by the loop DEI in the low T_e plasma (T_e=10 eV). In contrast with the above case, in the high T_e plasma (T_e=1.6 keV) the trajectory of X-mode, DJ, deviates a little from that of cold one and the Bernstein wave propagates along the curve, GLK, and the exact trajectory is given by the hooked nail curve DJK. It is noted that points A, B, C, ... on the trajectories in Figs. 3(b) and (c) correspond to those A, B, C, .., respectively, on the dispersion curves in Fig. 2.

Solving eq.(3) and its derivative $\partial\varepsilon/\partial k_\perp = 0$ simultaneously, the approximate equations for ω_{pe}^2/ω^2 and $k_\perp \rho_e$ at the turning points of the Bernstein modes (H, O, L) are derived as functions of Ω_e/ω and $k_z \rho_e$. Then the direction of group velocity, $v_{gz} \gtrless 0$, at these points is determined by the following relation:

$$(k_z \rho_e)^2 \gtrless 2 \frac{\Omega_e^2}{\omega^2} \left\{ (1 - \frac{\Omega_e^2}{\omega^2})(\sum - 1)[1 + (1 - \frac{\Omega_e^2}{\omega^2})(\sum - 1)] \right\}^{-1}, \qquad (6)$$

with $\sum = [1 + 3(\Omega_e/\omega)^2][1 - (\Omega_e/\omega)^2]^{-3}$. While RHS of eq.(6) is

nearly constant, $k_z\rho_e$ increases with T_e, therefore v_{gz} becomes positive in high T_e plasmas. In fact, eq.(6) shows that $v_{gz} > 0$ if $T_e > 1.6$ keV for the plasma parameters in Fig. 3(a). It is noted, however, that in an intermediate T_e plasma ($T_e = 0.8$ keV), the trajectory is the hooked nail curve, DMN, though that of Bernstein wave is given by the curve GON, which has a negative v_{gz} at the turning point o.

Passing a loop or a hooked nail curve near the second turning point, the X-mode is converted to the Bernstein wave, which propagates in a backward wave for the x-direction toward the ECR layer. As T_e changes, their trajectories are varied and in the limit of $T_e = 0$, the trajectory becomes a perpendicular line, which is the same as that in the case of $T_e \neq 0$, but $k_z = 0$ (perpendicularly propagating Bernstein wave). When the cyclotron damping becomes appreciable, the wave trajectory is roughly parallel to $\vec{B}$. The hatched hill is the absorbed power rate per unit length along the trajectory RQ, which is given by $dP/d\ell = -2(\mathrm{Im}\, k)P$ with $\mathrm{Im}\, k = \mathrm{Im}\,\varepsilon/(\partial \mathrm{Re}\,\varepsilon/\partial\omega)|\vec{v}_g|$. Here $\mathrm{Im}\,\varepsilon$ is the imaginary part of eq.(3), where the term of $n = 1$ is dominant. On the trajectory, RQ, for $T_e = 400$ keV, the cyclotron damping becomes effective at the point R and the wave is damed away at Q, where the ratio of rf power at Q, P_Q, to that at R, P_R, is taken as $P_Q/P_R = 5\times10^{-3}$. In addition to this cyclotron damping, the collisional damping is included, then $\mathrm{Im}\,\varepsilon$ is given by the imaginary part of the following dispersion equation:[9]

$$\varepsilon(\omega, \vec{k}) = 1 - \frac{2\omega_{pe}^2}{k_\perp^2 v_{Te}^2}\left(1 + i\frac{\nu}{\omega}\right)\sum_{n=-\infty}^{+\infty}\frac{n\Omega_e}{\omega + i\nu - n\Omega_e}e^{-\lambda}I_n(\lambda) = 0, \qquad (7)$$

wher ν is the electron-ion collision frequency.

Numerical calculations show that the cyclotron damping is dominated in high temperature plasmas of $T_e > 100$ eV in Fig. 3(b). Further, the absorbed power rate becomes the maximum at the position, where the inverse cyclotron frequency is given by $\omega/\Omega_e \approx 1 + 2.6\, k_z \rho_e$, independently of $k_z \rho_e$. Thus, the wave is damped away and electrons are heated locally before the wave is transmitted to ECR layer, which is in contrast with the ressult that most energy of the wave absorbed at ECR layer ($\omega = \Omega_e$).[5] On the other hand, the Bernstein wave is damped away near UHR layer ($\omega = \omega_{UH}$) by the collisional damping in low temperature plasmas of $T_e < 100$ eV. The above saying seems to correspond to the experimental results that the wave absorption is effective at UHR layer in low T_e ($\sim$10 eV) plasma in Tuman-2,[2] where the collisional damping may be dominant, while the cyclotron damping near $\omega = \Omega_e$, $2\Omega_e$ is effective in high T_e ($\sim$400 eV) plasma in TM-3.[1]

On the calculation of wave trajectory, described above, it remains to be questionable that WKB approximation may be broken near the plasma cutoff and the first and the second turning points. However, it has been shown that the transmission efficiency at the plasma cutoff and also the mode-conversion efficiency at the first turning point are quite high.[10] Further, it was reported by Schuss et al.[15] that an X-mode, propagating perpendicularly to B in the direction of decreasing magnetic field, almost completely converts into a backward Bernstein mode near the UHR layer.

The results are summarized as follows: In a toroidal plasma the O-mode injected at the incident angle θ_{opt} can

propagate into a dense plasma ($\omega_{pe}^2/\omega > 1$), where the wave is converted to the X-mode. This mode propagates back to the UHR layer, where the wave is converted to the backward Bernstein mode during passing a loop or a hooked nail curve. At last, the wave is cyclotron or collision damped away and the local electron heating occurs in front of ECR layer. Using the above-described wave trajectories and cyclotron damping, experiments on ECH are now under study.

The authors wish to express their thanks to Professors H. Ikegami, K. Matsuura, K. Miyamoto and to members of ECH Study Group of JIPP T-II at Institute of Plasma Physics, Nagoya University, for their discussions.

References

1 V. V. Alikaev, G. A. Bobrorskii, V. I. Poznyak, K. A. Razumova, V. V. Sannikov, Yu. A. Sokolov and A. A. Shmarin, Sov. J. Plasma Phys. 2 212 (1976).

2 V. E. Golant et al., Soviet Phys.-Tech. Phys. 17 488 (1972).

3 J. C. Sprott, Phys. Fluids 14 1795 (1971).

4 R. A. Dandl et al., in Proceedings of the Fifth Inter. conf. on Plasma Physics and Controlled Nuclear Fusion Research, Tokyo, 1974 2 141 (IAEA, Vienna 1975).

5 A. C. England, J. C. Sprott, O. C. Eldrige, W. Namkung, F. B. Marcus and J. B. Wilgen, ORNL/TM-5425 (1976)(unpublished).

6 V. V. Alikaev and Yu. I. Arsenyev, Experimental and Theoretical aspect of heating in Toroidal Device, Grenoble 1976.

7 T. H. Stix, Phys. Rev. Letters 15 878 (1965).

8 V. E. Golant and A. D. Piliya, Sov. Phys.-Uspekhi 14 413 (1972).

9 V. M. Kochetkov, Sov. Phys.-Tech. Phys. 21 280 (1976).

10 J. Preinhaelter and V. Kopecky, J. Plasma Physics 10 1 (1973).

11 J. Hosea, V. Arunasalam and R. Cano, Phys. Rev. Letters 39 408 (1977); A. E. Costley and TFR Group, ibid. 38 1477 (1977).

12 T. H. Stix, Theory of plasma waves (McGrow Hill, New York, 1962).

13 S. Ichimaru, Basic principles of plasma physics, Chap. 5 (Benjamin, Reading, Massachusetts, 1973).

14 S. Tanaka et al., Phys. letters 59A 290 (1976).

15 J. J. Schuss and J. C. Hosea, Phys. Fluids 18 727 (1975).

Figure Captions

Fig. 1 Refractive index $N_\perp$ perpendicular to magnetic field as function of plasma density (ω_{pe}^2/ω^2) for various values of N_z at a fixed value of magnetic field $(\Omega_e/\omega = 2/3)$. Solid and dotted curves show the extraordinary (X) and the ordinary (O) modes, respectively.

Fig. 2 Refractive index $N_\perp$ versus plasma density (ω_{pe}^2/ω^2) for the optimum $N_{z,opt}=0.6325$ ($\theta_{opt}= 51$ deg) at the fixed value of $\Omega_e/\omega=2/3$. For $T_e= 1.6$ keV, the exact dispersion curve calculated from eq.(2) is plotted by the solid one (ABCDJK), while the dispersion of cold X-mode calculated from eq.(1) is the dotted one (ABCDF) and that of Bernstein mode calculated from eq.(3) is the thin one (BGLK).

Fig. 3 (a) Electron density and field intensity variations in toroidal plasma. $\omega_{pe}^2(0)/\omega^2= 1.21$, $\Omega_e(0)/\omega = 0.87$ and $R/a = 91/17$ (for example $\Omega_e(0)/2\pi = 35$ GHz, $k_z = 5.63$ cm^{-1}, $a = 17$ cm and electron-ion collision frequency $\nu/\omega_{pe}(0) = 5.2\ 10^{-5}$, $2.1\ 10^{-6}$, $3.0\ 10^{-7}$, $4.2\ 10^{-8}$ for $T_e = 0.01$, 0.1, 0.4, 0.8 and 1.6 keV, respectively).

(b) and (c) Wave trajectories for $N_{z,opt} = 0.668$ in toroidal plasma with T_e as a parameter. For $T_e = 10$ eV, the exact trajectory calculated from eqs.(2) and (4) is plotted by the curve (ABCDEI), while the trajectory of cold X-mode calculated from eq.(1) is the curve (ABCDF) and that of Bernstein mode calculated from eq.(3) is the curve (GHI). The exact trajectories are plotted by curves (ABCDMN) and (ABCDJK) for $T_e = 0.8$ and 1.6 keV, respectively.

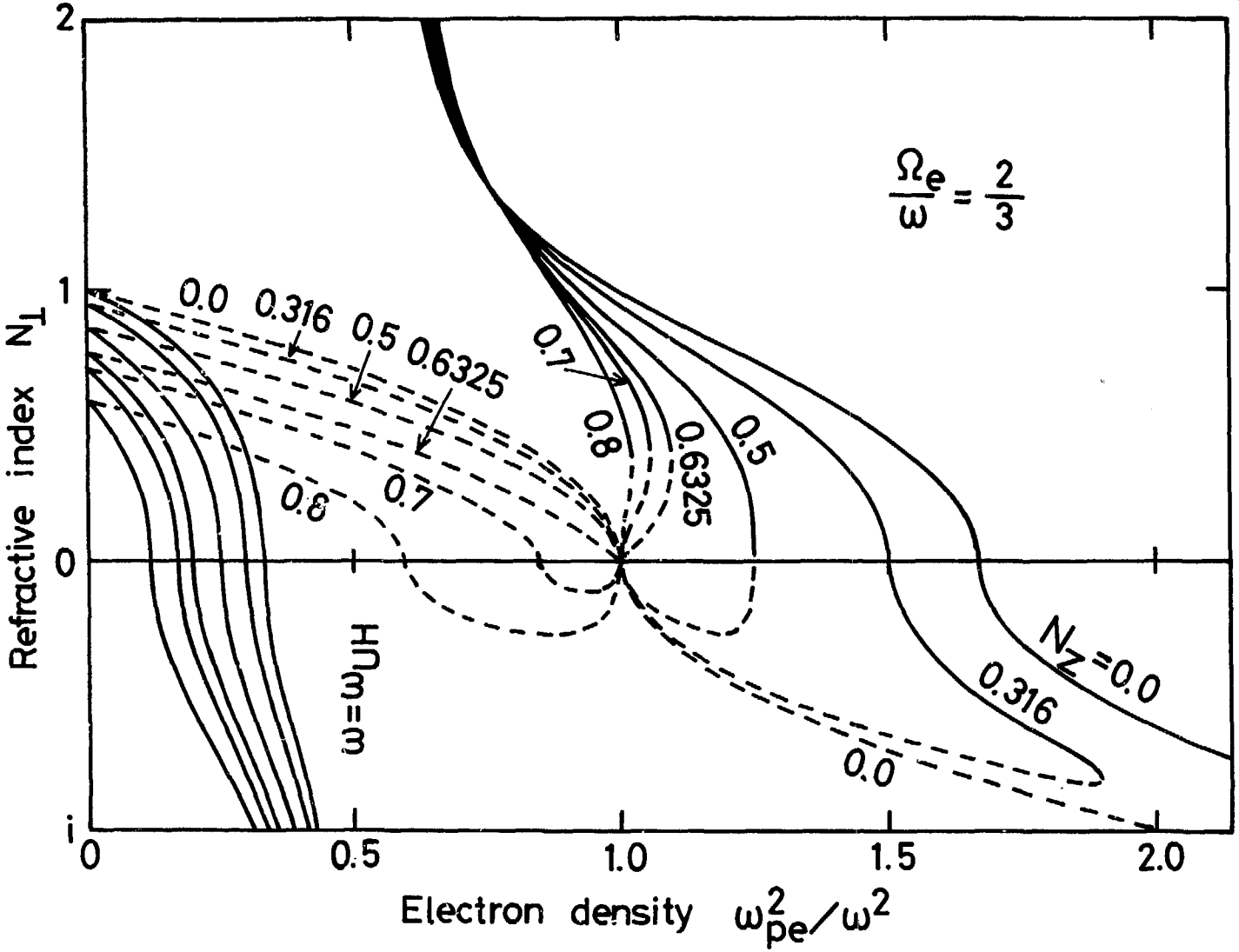
2
1
0
i
0
0.5
1.0
1.5
2.0
Refractive index $N_\perp$
Electron density ω_{pe}^2/ω^2
$\frac{\Omega_e}{\omega} = \frac{2}{3}$
$\omega = \omega_{UH}$
N_z =0.0
0.316
0.5
0.6325
0.7
0.8
0.0
0.316
0.5
0.6325
0.7
0.8

Fig. 1

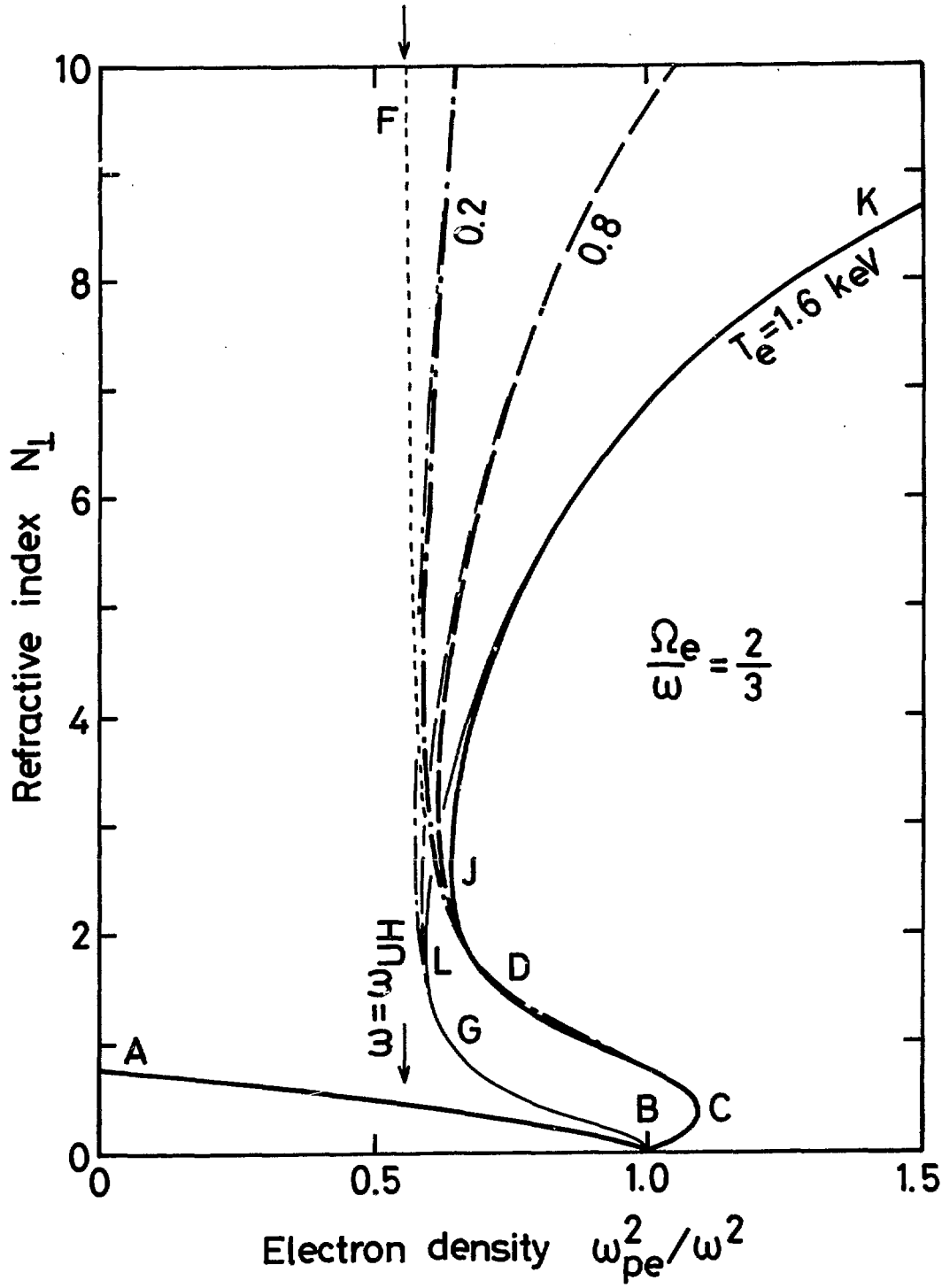
10
8
6
4
2
0
0
0.5
1.0
1.5
Refractive index $N_\perp$
Electron density ω_{pe}^2/ω^2
F
0.2
0.8
K
T_e=1.6 keV
$\frac{\Omega_e}{\omega} = \frac{2}{3}$
J
L
D
G
A
B
C
$\omega = \omega_{UH}$

Fig. 2

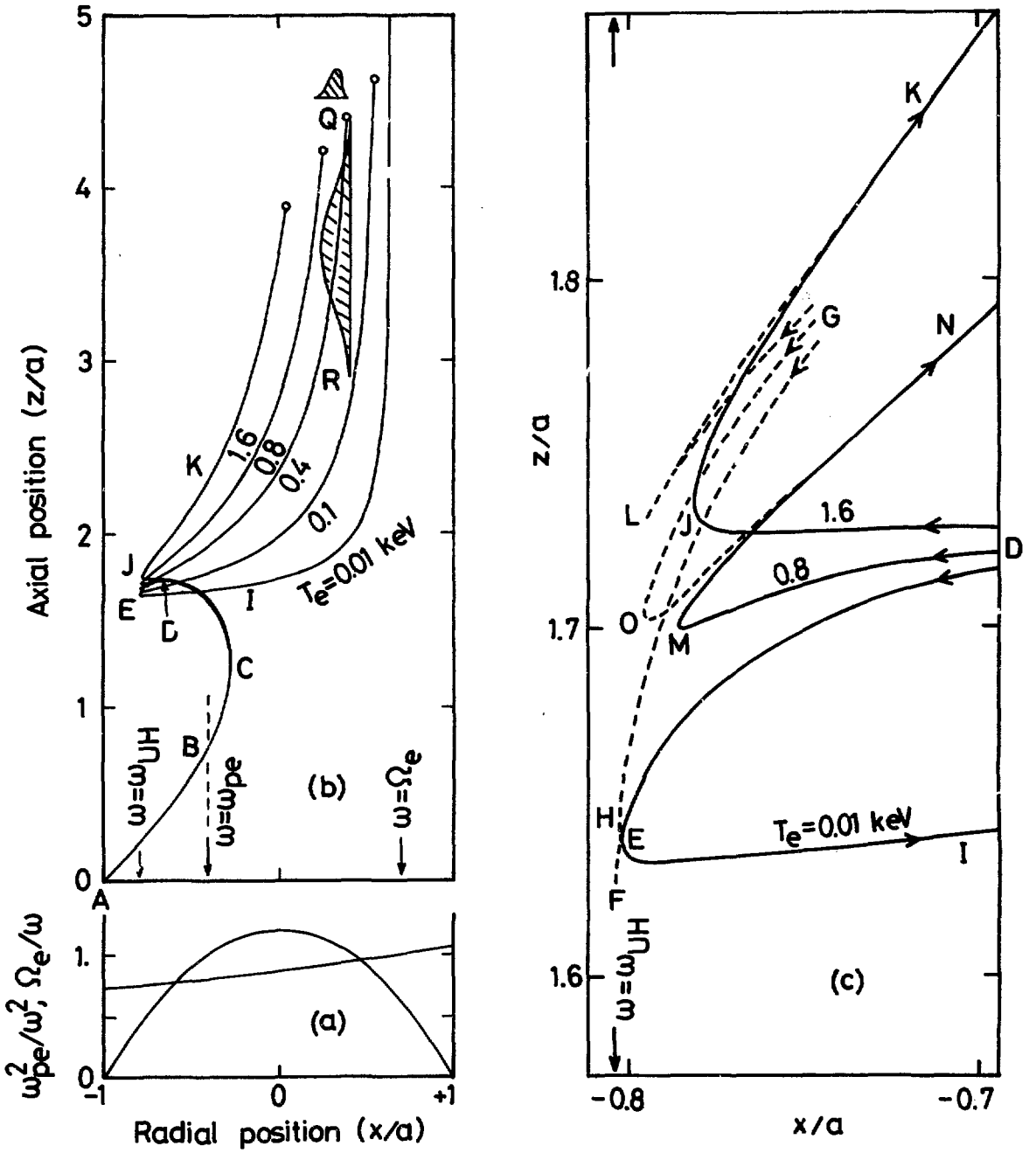
Axial position (z/a)
Radial position (x/a)
ω^2_{pe}/ω^2; Ω_e/ω
z/a
x/a
K
Q
R
1.6
0.8
0.4
0.1
J
E
D
I
C
B
A
T_e=0.01 keV
$\omega=\omega_{UH}$
$\omega=\omega_{pe}$
$\omega=\Omega_e$
(a)
(b)
(c)
G
N
L
O
M
H
F
1.8
1.7
1.6
-0.8
-0.7
-1
0
+1
1.

Fig. 3